Volume 27
Number 21
7 June 2025
Pages 3395–3606

CrystEngComm

rsc.li/crystengcomm

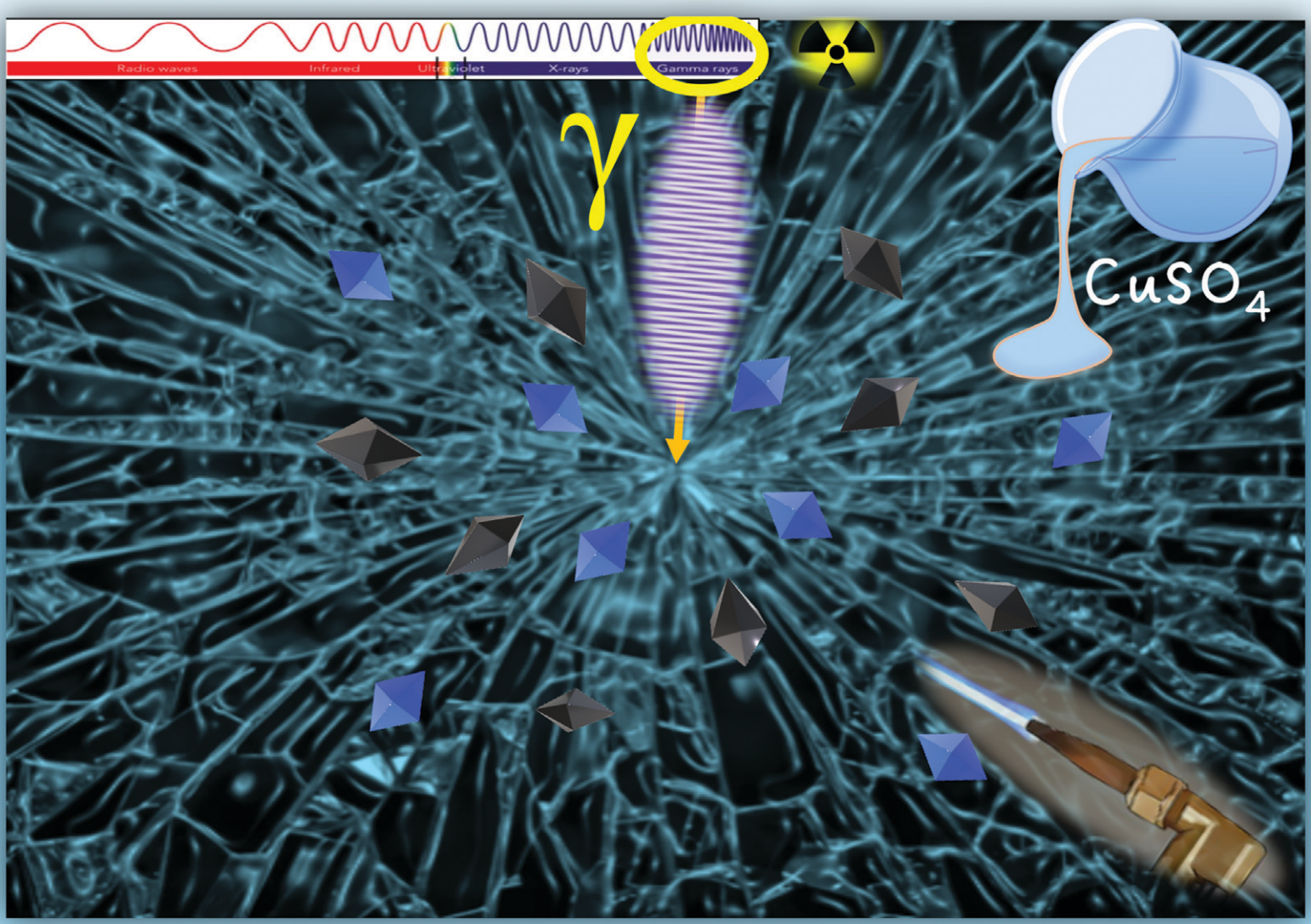

ISSN 1466-8033

PAPER

Alaa Adawy *et al.*

Embedding crystalline Cu and Cu_2O nanoparticles in silicate glasses through an ion-exchange process followed by gamma irradiation and annealing: an optical absorption spectroscopy assessment

ROYAL SOCIETY OF CHEMISTRY

CrystEngComm

PAPER

View Article Online
View Journal | View Issue

Cite this: *CrystEngComm*, 2025, **27**, 3444

Embedding crystalline Cu and Cu_2O nanoparticles in silicate glasses through an ion-exchange process followed by gamma irradiation and annealing: an optical absorption spectroscopy assessment

Safa Toumi, [a] Khaled Farah*[bc] and Alaa Adawy *[de]

Studies focusing on finding methodologies to obtain nanocrystalline structures in the form of nanoparticles have gained significant interest in the last two decades, given their broad possibilities to serve in different technological applications, and those related to glass technology are not an exception. Different routes are utilized to characterize crystalline nanoparticle growth. Hereby, an ion-exchange process followed by gamma ray irradiation and/or annealing treatment was used to effectuate the growth of copper nanoparticles (CuNPs) in glass matrices. Relying on well-established optical absorption spectroscopy, a precise and timely analysis of the changes occurring in the glass matrix, along with the formation of the CuNPs, defining their oxidation state and their sizes was performed. The study revealed that the formation of CuNPs in the glass matrix takes place within an unexpectedly short duration after the ion-exchange process. Irradiating the Cu-exchanged glass with gamma rays at ≈100 kGy increased the CuNPs formation and volume fraction, whereas at higher doses ≈1000 kGy the formed nanoparticles had smaller sizes. Interestingly, combining γ-irradiation with annealing for the Cu-exchanged glasses resulted in either size growth of CuNPs or their partial or total oxidation and their conversion to the more stable and ecofriendly Cu_2O nanoparticles.

Received 4th December 2024,
Accepted 1st April 2025

DOI: 10.1039/d4ce01225a

rsc.li/crystengcomm

1. Introduction

Glass silicates that contain nanoparticles of copper, silver and gold exhibit nonlinear optical properties and thus they have high potential to be used across several applications.[1,2] They have been widely used for glass coloration,[3] for ionizing radiation dosimetry,[4,5] and for fabricating optical devices, such as waveguides, lenses, and optical switches.[6–8] There are several methodologies employed for incorporating noble metals into a glass surface,[9–11] among which is the ion-exchange process given its simplicity and minimal equipment requirements.[12] Combining heat treatment with ion-exchange has attracted great interest, owing to their potential to embed nanoscale metallic particles in glass silicates such as copper nanoparticles (CuNPs), which have been widely studied, because of their unique optical responses in the wavelength range of 560–570 nm that are attributed to the well-known surface plasmon resonance (SPR).[13,14] In fact, SPR is crucial for numerous linear and nonlinear applications, making the optical response of CuNPs essential for their use in surface plasmon-based components. SPR provides information on the composition and particle size, since the position and shape of the SPR band are influenced by the structure and distribution of the clusters, as well as the dielectric properties of metal. Irradiation with electromagnetic waves such as lasers, gamma rays, electrons, heavy ions or X-rays accompanied by or used instead of heat treatment is nowadays an accepted approach for producing metallic nanoclusters post ion-exchange in glass silicates. Ionizing radiation results in modifications in the chemical, electrical, mechanical, magnetic, and/or optical properties of glass, due to the defect formation in the vitreous matrix

[a] *Laboratory of Physico-Chemistry of Materials (LPCM), Physics Department, Faculty of Sciences of Monastir, University of Monastir, Tunisia*
[b] *Higher Institute of Transport and Logistics of Sousse, University of Sousse, 4023, Tunisia*
[c] *Research Laboratory on Energy and Matter for Nuclear Science Development (LR16CNSTN02), National Centre for Nuclear Science and Technology, Sidi Thabet, 2020, Tunisia. E-mail: k.farah@cnstn.rnrt.tn*
[d] *Department of Physics, Faculty of Science, University of Oviedo, 33007 Oviedo, Asturias, Spain. E-mail: hassanalaa@uniovi.es*
[e] *Unit of Electron Microscopy and Microprobe, Institute for Scientific and Technological Resources (SCTs), University of Oviedo, 33006, Oviedo, Asturias, Spain*

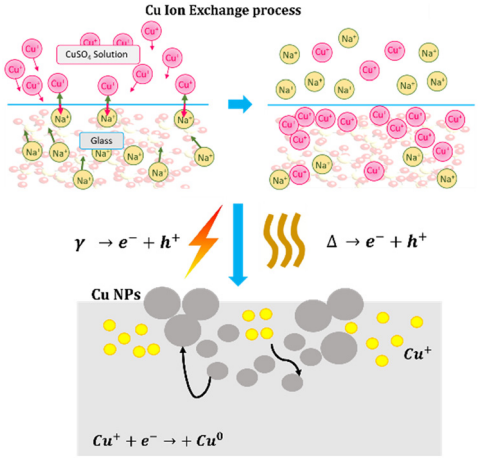

Fig. 1 Schematic representation for the Cu ion-exchange process and growth of Cu NPs inside the glass matrix.

structure. The production of these defects causes preferential light absorption at specific wavelengths, rendering the translucent glass coloured, creating the so called "colour centres". There are many types of these centres depending on the glass composition.

Many studies have explored the combined effects of ionizing radiation and heat treatment on the formation of silver nanoparticles (AgNPs) in ion-exchanged glass.[14–16] Additionally, proton irradiation effects on silicate glass have been studied in our previous paper.[17] However, only a few studies have been reported about the dual role of gamma irradiation and heat treatment on the formation of CuNPs in ion-exchanged glass. The main goal of the present work is to study the optical absorption properties of copper nanoclusters embedded in the Cu^{+}–Na^{+} ion exchanged soda-lime glass post heat treatment and gamma irradiation. Our studies indicate that the first stage of CuNPs formation occurs within a short duration of the ion-exchange process. Particularly, the dual heat treatment and gamma irradiation resulted in either the CuNPs growth or the partial to total oxidation of copper, resulting in the formation of Cu_2O nanoparticles (Fig. 1).

2. Experimental section

The glass samples were obtained from a single glass sheet, to ensure their structural similarities, and were cut into pieces with dimensions of 11 × 30 × 1.5 mm^3. The chemical composition of the glass samples in weight% is: 68.52 SiO_2, 13.77 Na_2O, 8.19 CaO, 4.34 MgO, 1.003 Al_2O_3, 0.588 K_2O, 0.105 Fe_2O_3 and about 3.5% of other components.[18]

For the ion-exchange treatment, the glass samples were dipped in a molten salt bath formed by mixing 10 g of copper and sodium; (54 : 46 mol%), at 550 °C, for 15 minutes. The ion-exchanged samples were then removed from the bath at room temperature, cleaned with distilled water to remove the adhering residues to their surfaces, and finally air dried on dust-free paper. The generated copper-exchanged glass samples were then irradiated at the Tunisian pilot plant ^{60}Co gamma irradiation facility[19] at room temperature with doses varying from 1 to 1000 kGy. The thermal annealing was done in an electrical furnace in atmospheric air. The as-exchanged non-irradiated and irradiated samples at 1000 kGy were annealed at 600 °C for different time periods ranging from 30 to 180 min. On the other hand, the Cu-exchanged and irradiated samples at 100 kGy were annealed for 30 min at a large temperature range from 60 to 500 °C. The details of every sample's experimental conditions are displayed in Table 1.

The optical absorption (OA) spectra were measured in the range of 300–700 nm by using a Shimadzu UV-vis spectrophotometer (model PharmaSpecUV-1700). The measurements were conducted against those of a glass sample that neither had undergone ion exchange nor gamma irradiation as the control sample (G-blank). The Electron Paramagnetic Resonance (EPR) spectra of the Cu-exchanged irradiated and annealed samples were measured at room temperature using a Bruker ER-200D spectrometer located at CNSTN, Tunisia. The spectrometer operates at 9.8 GHz X-band frequencies with a modulation amplitude of 0.2 mT, modulation frequency set at 100 kHz, a sweep width of 210 mT, and a microwave power of 63 mW. The high-resolution transmission electron microscopy and related crystallographic and size analyses were performed on JEOL-

Table 1 The labels of the samples

Sample	Treatment	Dose (kGy)	Annealing temperature (°C)/duration (min)
G-Blank	—	—	—
G-EXC	Ion-exchange (IE)	—	—
G-A600-30	IE + annealing	—	600 °C/30 min
G-A600-60	IE + annealing	—	600 °C/60 min
G-A600-180	IE + annealing	—	600 °C/180 min
G-I1	IE + irradiation	1	—
G-I10	IE + irradiation	10	—
G-I100	IE + irradiation	100	—
G-I1000	IE + irradiation	1000	—
G-IA100	IE + irradiation + annealing	100	60–500 °C/30 min
G-IA1000-30	IE + irradiation + annealing	1000	600 °C/30 min
G-IA1000-60	IE + irradiation + annealing	1000	600 °C/60 min
G-IA1000-180	IE + irradiation + annealing	1000	600 °C/180 min

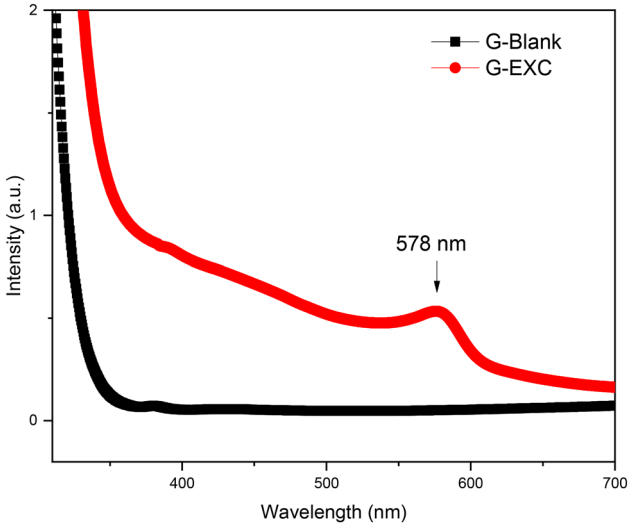

Fig. 2 Optical absorption spectra of G-Blank (black curve) and G-EXC (red curve).

JEM 2100F with characteristics and experimental setup thoroughly detailed elsewhere.[20]

3. Results

3.1. Effect of ion-exchange

Fig. 2 reveals the optical absorption spectra of the G-Blank and the G-EXC samples. A broad absorption peak centred around 578 nm is observed in the ion-exchanged glass, which accounts for the surface plasmon resonance band of the CuNPs.[21,22] The Cu^{+}–Na^{+} ion exchange of the glass at 550 °C for 15 minutes resulted in the formation of a small number of elemental Cu^{0} within the glass matrix.

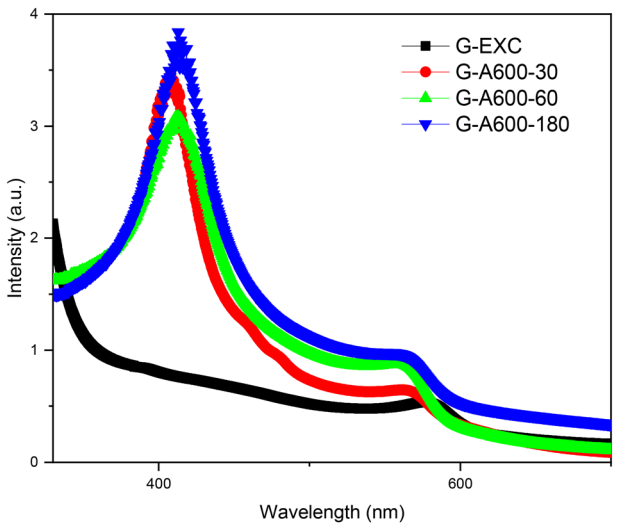

Fig. 3 Optical absorption spectra of G-EXC before (black curve) and after the annealing treatment at 600 °C for different durations [30 (red curve), 60 (green curve) and 180 (blue curve) minutes].

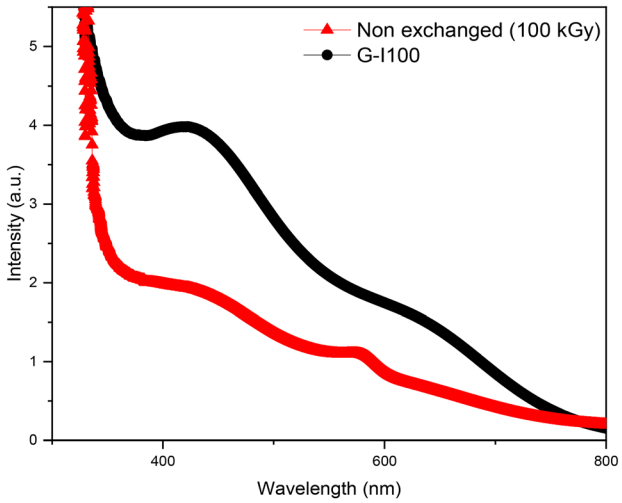

Fig. 4 Optical absorption spectra of the non-exchanged glass (red curve) and the Cu-exchanged glass (black curve) after being irradiated at 100 kGy.

3.2. Effect of annealing treatment

The ion-exchange process was followed by an annealing treatment in atmospheric air at 600 °C for 30, 60 and 180 minutes. The optical absorption spectra of the annealed samples for different durations are shown in Fig. 3. A notable increase in the SPR peak intensity (around 578 nm) was observed upon increasing the atmospheric post heat-treatment time, indicating a rapid increase in the number of Cu^{0} atoms on the surface of the Cu ion exchanged glass matrix.

For the annealed samples G-A600-30, -60 and 180, a notable blue-shift of the SPR band position could be observed, compared to the G-EXC sample (Fig. 2). This plasmonic peak shift accounts for a change in the cluster size.[23] Beside this peak, another sharp peak could be detected between 350 and 450 nm, which is attributed to the presence of Cu_2O nanoparticles.[24] The longer the duration of heat treatment, the higher the amplitude of this absorbance peak.

3.3. Effect of gamma irradiation

The G-Blank and G-EXC samples were exposed to gamma rays at 100 kGy. Optical absorption spectra of both samples are shown in Fig. 4. The non-exchanged, but irradiated sample's spectrum displays an overlapping of two characteristic bands with maxima at about 410 and 630 nm that are attributed to non-bridging oxygen hole centres (NBOHCs) type HC_1 and type HC_2, respectively.[25] The

Table 2 Gaussian fitting parameters of the optical spectrum of the non-exchanged glass sample irradiated at 100 kGy

Peak position (nm)	FWHM (nm)	Area under the band	Assignment
410	230.57	938.74	HC_1
628	158.81	175.9	HC_2

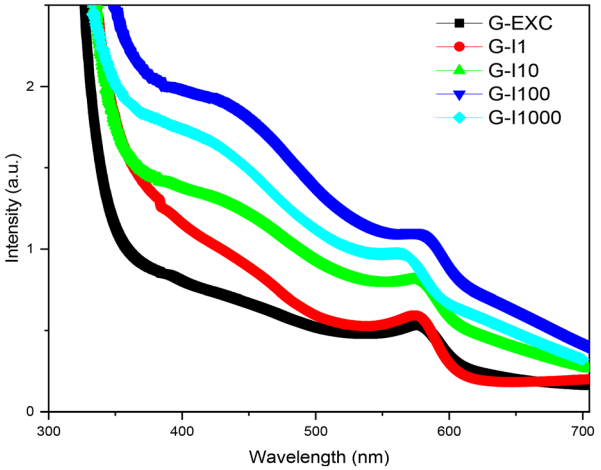

Fig. 5 Optical absorption spectra for the Cu-exchanged (black curve) and the irradiated samples with doses of 1 kGy (G-I1, red curve), 10 kGy (G-I10, green curve), 100 kGy (G-I100, blue curve) and 1000 kGy (G-I1000, baby blue curve).

spectrum was fitted by Gaussian curves, for which the fitting parameters are displayed in Table 2. Following the Cu ion-exchange treatment, a significant reduction in the optical absorption response of the irradiated glass was observed. This reduction was accompanied by the appearance of a surface plasmon resonance (SPR) peak, which was already detected in the spectra of the G-EXC and the annealed samples (Fig. 2 and 3).

According to previous studies,[26–29] the ionizing radiation leads to the formation of NBOHC defects in silicate glasses. These defects are typically classified into two categories, HC_1 and HC_2, both of which are paramagnetic and contribute significantly to the optical absorption spectra of irradiated glasses. Their formation originates from radiation-induced electron–hole pair generation, where holes are preferentially trapped by non-bridging oxygen atoms, forming NBOHCs, while electrons diffuse throughout the glass network. Wang *et al.* have further confirmed the presence of HC_1 (404–410 nm) and HC_2 (599–605 nm) absorption bands in multi-component glasses subjected to 1 MeV electron irradiation, with evidence supported by EPR measurements.[30]

3.4. Effect of absorbed doses

To investigate the effect of varying irradiation doses on the optical absorption spectra of the as-exchanged glass and especially on the evolution of the SPR peak, the Cu-exchanged samples were irradiated in a large dose range of 1–1000 kGy (Fig. 5). It could be observed that irradiating the Cu-exchanged samples with doses up to 100 kGy resulted in a notable increase in the NBOHC absorption band (410 nm) and the SPR peak intensity. However, once the exposure reaches 1000 kGy, a notable decrease has been observed accompanied by a remarkable blue-shift of about 15 nm in the SPR absorption peak. In the present study, the average cluster radii (R) were determined from the full width at half maximum $\Delta\lambda$ (FWHM) of the optical absorption peaks using the following equation:[21,22]

$$R = \frac{V_f {\lambda_p}^2}{2\pi C \Delta\lambda} \quad (1)$$

where $V_f = 1.57 \times 10^6$ m s^{-1} is the Fermi velocity for bulk copper, $\Delta\lambda$ is the full width at half maximum of the absorption band and λ_p is the specific wavelength at which SPR takes place. It is worth mentioning that the SPR peak

Table 3 Approximated cluster sizes, SPR peak positions and the FWHM for the Cu-exchanged and the irradiated samples from 1 up to 1000 kGy

Sample	Peak position (nm)	FWHM (nm)	Size (nm)
G-EXC	577.3	30.8	8.56
G-I1	575.1	37.7	7.01
G-I10	575.7	46	5.76
G-I100	574.5	85.2	3.09
G-I1000	563.4	192.5	1.31

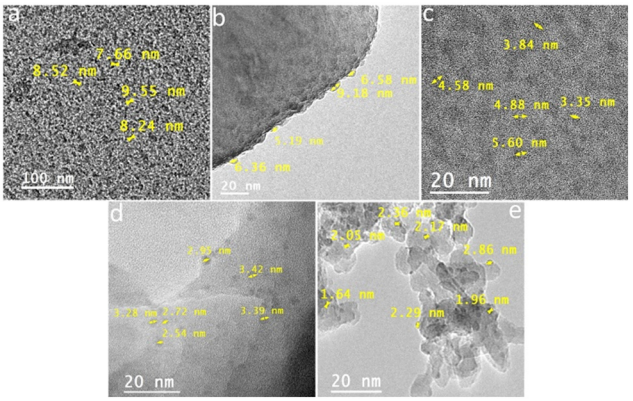

Fig. 6 HRTEM images for the Cu-exchanged (a) and the irradiated samples with doses of 1 kGy (G-I1, b), 10 kGy (G-I10, c), 100 kGy (G-I100, d) and 1000 kGy (G-I1000, e).

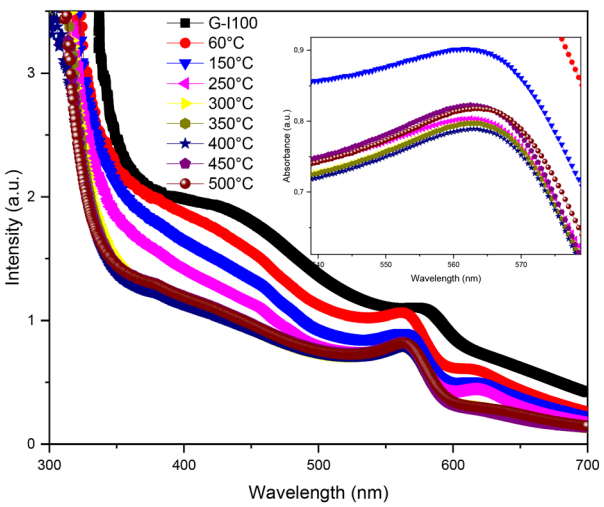

Fig. 7 Optical absorption spectra for G-I100 before the annealing treatment and after annealing (G-IA100) at temperatures between 60 and 500 °C. The inset shows a magnification for the obtained spectra in the wavelength range between 540–580 nm.

position and the plasmon bandwidth were obtained by using a bi-Gaussian function to fit the experimental absorbance plots, commonly employed for asymmetric peaks.[31] Based on the acquired spectra, the size of the formed CuNPs was found to significantly decrease with increasing the irradiation dose (Table 3). This estimation was in accordance with the high-resolution transmission electron microscopy (HRTEM) inspection for the respective samples in which we observed similar size ranges of the formed nanoclusters (Fig. 6).

3.5. Effect of gamma irradiation and heat treatment

3.5.1 Gamma rays + isochronous annealing. The glass samples that were gamma irradiated at 100 kGy and annealed at different temperatures ranging from 60 °C to 500 °C for 30 minutes showed the combined effects on Cu-exchanged glass (Fig. 7). The optical absorption spectrum of the Cu-exchanged irradiated sample (G-I100) before annealing showed the NBOHC (HC_1 and HC_2) bands at about 440 and 630 nm, along with the SPR peak of CuNPs. Significant reduction in optical absorption intensity has been observed immediately after initiating the annealing treatment (60 °C). Increasing the temperature up to 300 °C resulted in a decrease in the absorbance that in turn remained constant up to an annealing temperature of 500 °C. The size of CuNPs increased with increasing temperature, reaching a maximum value at 350 °C, followed by a slight decrease (Table 4).

Fig. 8 shows the Electron Paramagnetic Resonance (EPR) spectra of the gamma-irradiated sample at 100 kGy, followed by an annealing treatment for 30 minutes at various temperatures ranging from 60 °C to 500 °C. The G-I100 sample exhibited an EPR signal in the 3500–3550 G range (g_1 = 1.995, g_2 = 1.990, g_3 = 1.988), which is attributed to the NBOHC defect, similar to those previously reported in various other glasses.[32,33]

It is worth noting that both HC_1 and HC_2 defects are characterized by their overlapping EPR resonance associated with the same fundamental paramagnetic centre (NBOHC), a signal that is a superposition of two components attributed to HC_1 and HC_2. Furthermore, detailed EPR studies showed that although HC_1 and HC_2 gave rise to distinct optical absorption bands, they are not separate species but rather variants of the same NBOHC defect with slightly different local environments. Notably, distinguishing between HC_1 and HC_2 components remains challenging due to their close spectral overlap.[30,34]

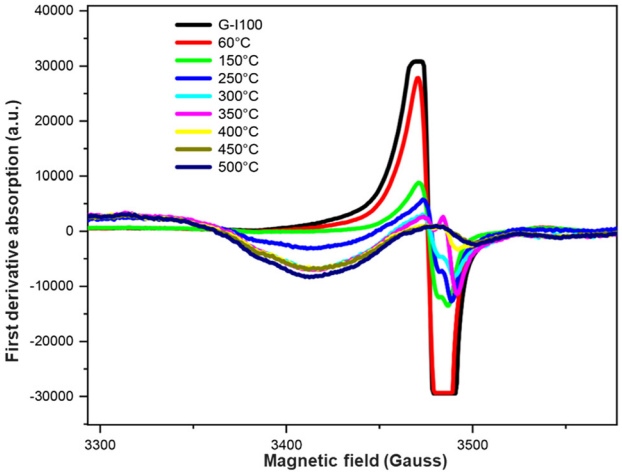

Fig. 8 EPR spectra for G-I100 before the annealing treatment and after annealing (G-IA100) at temperatures between 60 and 500 °C.

As the annealing temperature increased, the intensity of the NBOHC signal decreased, while a characteristic Cu^{2+} signal appeared in the 3400–3450 G range, (g-values: $g_{\|}$ = 2.232 and $g_{\perp}$ = 2.040). This signal, attributed to Cu^{2+} ions, is consistent with previous reports in various copper doped glass matrices.[35,36] With further annealing, the intensity of this Cu^{2+} signal gradually increased, suggesting a concurrent decrease in the presence of monovalent Cu^{+} ions, which are diamagnetic and therefore do not contribute to EPR signals.[37]

3.5.2 Gamma rays + isothermal annealing. Fig. 9 shows the UV-vis spectra of the Cu-exchanged samples irradiated at 1000 kGy and annealed at 600 °C for 30, 60, and 180 minutes. Annealing the irradiated sample for 30 minutes at 600 °C resulted in a slight decrease in the SPR peak intensity

Table 4 Approximated average cluster sizes, SPR peak positions and the FWHM for the annealed samples at various temperatures up to 500 °C for a duration of 30 min

Annealing temperature (°C)	Peak position (nm)	FWHM (nm)	Radius (nm)
Un-annealed	574.5	85.2	3.09
60	563.6	63	4.02
150	563.5	38.8	6.53
250	564.2	40	6.54
300	564.1	34.3	7.42
350	563.5	31.9	7.96
450	563.7	32.4	7.84
500	564.5	34	7.49

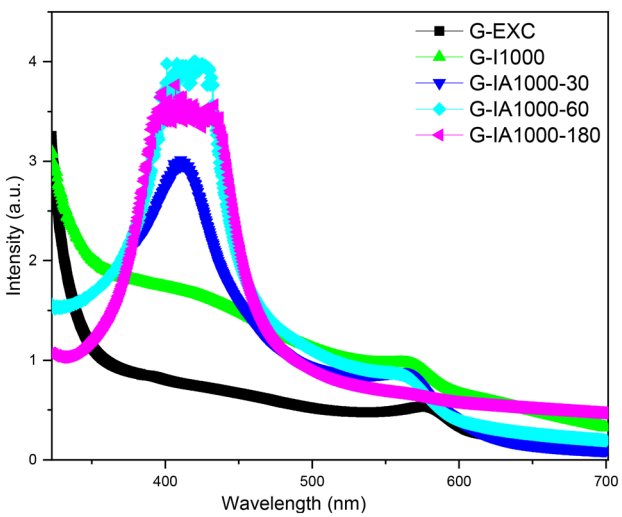

Fig. 9 Optical spectra of G-EXC (black), G-I1000 (green) and the annealed irradiated samples G-I1000-30 (blue), G-I1000-60 (baby blue) and G-I1000-180 (pink).

and the onset of the Cu_2O NP band. Increasing the heat treatment duration to 60 min resulted in a decrease in the SPR peak that became barely visible, while the band at 490 nm significantly increased and reached a maximum, indicating further oxidation of CuNPs. Upon extending the annealing duration to 180 minutes, the absorbance band of Cu_2O NPs decreases and reaches a plateau region of constant absorbance from 390 to 440 nm, while the SPR peak completely disappears.

The crystallographic analysis of the HRTEM images acquired for the glass exchanged sample and those that were afterwards irradiated and annealed showed the presence of only copper nanocrystals in the former and a mix of copper and Cu_2O nanocrystals in the latter (Fig. 10).

4. Discussion

In the Cu^+–Na^+ ion-exchanged glass matrix, copper diffuses into the glass matrix to a depth of a few microns.[38] The monovalent copper ions control the exchange process in silicate glass networks, along with a restricted direct exchange with divalent copper ions due to their notably low diffusion coefficient.[38,39] Indeed, during the ion exchange of Cu–Na, copper penetrates into the glass principally in the form of Cu^+ ions, replacing the Na^+ ions of the matrix as shown in eqn (2). The ion-exchange process is typically carried out by substituting Na^+ ions in sodium silicate and soda-lime glasses due to the high mobility and large molar concentration of Na^+ ions compared to other alkali ions present in the glass. The substantial presence of Na^+ ions allows an increased number of Cu^+ ions to penetrate the glass, making Na^+ the most promising candidate for ion exchange with copper.[40]

$$\equiv Si{-}O{-}Na^+ + Cu^+SO_4^- \rightarrow \equiv Si{-}O{-}Cu^+ + Na^+SO_4^- \quad (2)$$

Then, a small fraction of the diffused Cu^+ ions can be further reduced to elemental Cu^0 atoms, leading to the emergence of a surface plasmon resonance (SPR) peak in the G-EXC sample (Fig. 3). The reduction of Cu^+ to Cu^0 is facilitated by electrons originated from non-bridging oxygen (NBO) atoms within the glass matrix. It was found that the number of NBOs in the glass structure, determined by the content of network modifiers (*e.g.*, Na_2O, CaO), directly influences the ion mobility and diffusion rate.[41] Glasses with a higher NBO content, such as silicate glasses with sufficient Na_2O, facilitate faster diffusion, thereby enhancing the ion-exchange process and subsequent CuNP formation. These oxygen atoms provide the electrons necessary for the reduction process, enabling the formation of neutral copper atoms. As a result, a small number of metallic Cu clusters begins to form even during the ion-exchange phase. Similar findings have been reported in prior studies, where Cu-doped soda-lime glass exhibited an SPR band after undergoing a short ion-exchange process (~1 min) at 560–570 °C.[42]

In this study, the ion-exchange process was conducted at 550 °C for 15 minutes. This specific temperature was selected to ensure complete fusion of the salt mixture (54 : 46 mol%), a crucial factor for efficient ion exchange and controlled Cu nanoparticle (CuNP) formation. At lower temperatures, incomplete fusion was observed, resulting in insufficient ion exchange. Conversely, increasing the duration beyond 15 minutes led to the absence of the SPR band, likely due to excessive Cu diffusion which could result in the dissolution or oxidation of Cu species, preventing stable nanoparticle formation. This fact could explain the absence of the SPR band in the absorbance spectrum of the as-exchanged Cu sample in our previous study,[17] where the ion-exchange duration was four times longer than that in the current work.

The role of ion-exchange conditions in CuNPs formation is further confirmed in other previous studies.[43] UV-vis spectroscopy of samples subjected to a shorter ion-exchange process (5 minutes at 580 °C) revealed a broad, low-intensity SPR peak around 570 nm, indicative of the presence of very small CuNPs (at about 1 nm).[43] The weak SPR signal suggested either the early stages of nanoparticle nucleation where the particles were too small to display strong plasmonic interactions or a limited number of CuNPs prior to annealing. These findings emphasize the sensitivity of CuNPs formation to ion-exchange parameters, reinforcing the selection of 550 °C for 15 minutes as an optimal balance between nanoparticle stability and efficient ion exchange.

Another independent study supported this observation, demonstrating that even a 5 minute ion exchange treatment

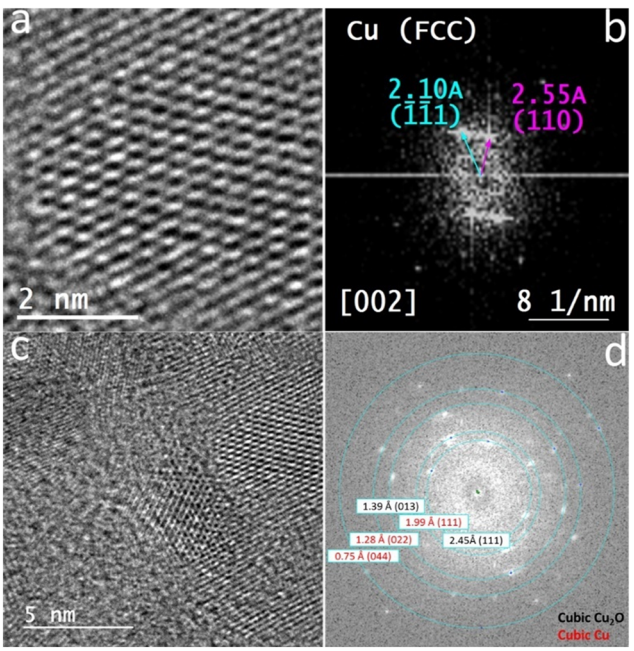

Fig. 10 Upper panel for the glass-exchanged sample: HRTEM image (a) and its crystallographically analysed fast Fourier transform [FFT] result, revealing the [002] plane of the cubic crystal of copper (b); lower panel for the glass-exchanged sample, 10^6 Gy irradiated and annealed at 600 °C for 60 minutes: HRTEM image (c) and its crystallographically analysed FFT result (d), revealing the fingerprints of cubic copper (red) and cubic Cu_2O (black) crystals.

could lead to the emergence of an SPR peak in Cu-exchanged glass samples.[21]

In our study, a notable increase in the SPR peak intensity was observed upon increasing the atmospheric post heat-treatment duration (Fig. 2). This enhancement accounts for a rapid increase in the number of elemental Cu^0 atoms on the surface of the Cu-exchanged glass matrix. It has been previously reported that the number of reduced Cu^0 increases with increasing annealing temperatures and when using longer heat treatment durations.[21,44] This leads to an increase in the number and dimension of Cu aggregates near the surface of the glass matrix. Indeed, the thermally annealed samples have a higher number of free electrons when compared to the Cu-exchanged sample.[44,45] As a result, many Cu^+ ions can trap these electrons and form copper atoms (Cu^0) near the surface of the glass matrix. Typically, the post-thermal treatment process of the Cu-exchanged glass samples promotes the reduction of Cu^+/Cu^{2+} to elemental Cu^0 atoms after capturing the electrons from the glass structure or impurities as follows:

$$\text{Glass} \xrightarrow{\text{heating}} e^- + h^+ \quad (3)$$

$$Cu^+ + h^+ \rightarrow Cu^{2+} \quad (4)$$

$$Cu^{2+} + e^- \rightarrow Cu^+ \quad (5)$$

$$Cu^+ + e^- \rightarrow Cu^0 \quad (6)$$

$$mCu^0 \Rightarrow (Cu^0)m \quad (7)$$

where, h^+ is a hole, e^- is an electron, and m is the number of Cu atoms forming the nanoparticles.

The notable blue-shift of the SPR band position that was observed as the annealing duration increased (Fig. 3) is generally attributed to a change in the cluster size. In earlier studies, a similar kind of blue shift in the SPR peak after the heat treatment process of the Cu-exchanged glass sample was reported and attributed to a significant reduction in nanoparticle size.[23,24,44] Moreover, the formation of Cu_2O NPs was confirmed by the appearance of a characteristic absorption band between 350 and 450 nm.[24] The absorbance intensity was significantly higher for the samples subjected to a longer heat treatment duration. This indicates that annealing the Cu-exchanged glass sample at 600 °C in air promotes the growth of Cu_2O NPs. Indeed, the diffusion of oxygen atoms into the near-surface of the Cu-doped layer in the soda lime glass results in the partial oxidation of copper ions to form Cu_2O NPs on the surface of the glass matrix, resulting in a mixture of both phases within each particle. This transformation could take place according to the following equation:

$$2Cu + 1/2O_2 \rightarrow Cu_2O \quad (8)$$

Similar oxidation of CuNPs in air was previously reported in a study focused on the synthesis of CuNPs possessing a size of 2–65 nm in a silica matrix by a sol–gel technique.[24] The previous study highlighted the onset of the Cu_2O NP band in the absorption spectra of the samples annealed in air (450–475 nm), along with a surface plasmon resonance (SPR) absorption peak, which was found to be blue shifted by lowering the temperature from 293 K to 77 and 4.2 K. Their investigation revealed that the nanoparticle size is influenced by annealing conditions: small particles (2–15 nm) grow in samples annealed in atmospheric air, medium-sized particles (15–40 nm) in samples annealed first in air and then in molecular hydrogen, and large particles (40–65 nm) in samples annealed in molecular hydrogen. The feature of the Cu_2O NP band was found to be influenced by the size of the formed CuNPs. A sharp peak was only observed in the presence of small CuNPs formed during annealing in atmospheric air, while for larger CuNPs, the band was barely detectable. It is worth mentioning here that the kinetics of the oxidation process could be also influenced by the size of CuNPs. Generally, the smaller the CuNPs, the larger their surface area-to-volume ratio, which could improve their reactivity and further facilitate the formation of Cu_2O nanoparticles.

The effect of irradiation on the optical absorbance of both the G-Blank and G-EXC samples was also studied. Non-bridging oxygen hole centers (NBOHCs) of types HC_1 and HC_2 were detected at approximately 410 nm and 630 nm, respectively (Fig. 3). The NBOHC defects are paramagnetic and usually formed after exposure to ionizing radiation, dominating the optical spectra of glass silicates. Indeed, the formation of NBOHC defects in glass upon its irradiation starts with the formation of electron–hole pairs. In silica-based glass, the holes are mostly trapped by the non-bridging oxygen atoms leading to the formation of NBOHCs, while electrons diffuse through the glass network.[46] The notable decrease in the optical absorption response of the irradiated glass could be explained by a significant decrease in the amount of the formed NBOHCs. This decrease was accompanied by the presence of an SPR peak, which was already detected in the spectra of the Cu-exchanged and annealed samples (Fig. 2 and 3). This finding is in agreement with an earlier result in previous research by our group,[33] in which we showed a sharp decrease in the EPR signal of the formed NBOHC ($\equiv$Si–O°) defects, and thus upon Cu ion-exchange. This decrease was accompanied by the appearance of an intense signal related to Cu^{2+} ions. This observation confirms that copper was introduced into the glass principally in the form of Cu^+ ions, acting as an electron trap, promoting the recombination of holes created by irradiation by the rupture of the $\equiv$Si–O–Si$\equiv$ bonds as follows:

$$\equiv Si–O–Si\equiv \xrightarrow{\text{gamma irradiation}} \equiv Si–O^\circ + Si^\circ \quad (9)$$

$$Cu^+ + \equiv Si–O^\circ \rightarrow Cu^{2+} + \equiv Si–O^- \quad (10)$$

The optical absorption spectra of the Cu-exchanged glass samples were investigated as a function of the absorbed dose to understand the influence of dose variation on the

evolution of the SPR peak (Fig. 5). It was found that after the irradiation of the Cu-doped sample with doses up to 100 kGy, a notable increase in the NBOHC absorption band (410 nm) as well as in the SPR peak intensity was detected. It is worth noting that the higher intensity of the plasmonic peak suggested a greater volume fraction of CuNPs embedded in the glass matrix.[43] This effect could be assigned to the dominance of the conversions displayed in the following equations:

$$\text{glass} \xrightarrow{\text{gamma irradiation}} e^- + h^+ \quad (11)$$

$$Cu^{2+} + e^- \rightarrow Cu^+ \quad (12)$$

$$Cu^+ + e^- \rightarrow Cu^0 \quad (13)$$

$$mCu^0 \rightarrow (Cu^0)m \quad (14)$$

However, when the exposure dose reached 1000 kGy, a significant decrease in the SPR peak intensity was observed, accompanied by a clear blue-shift of about 15 nm in the SPR absorption peak. In another study, a similar shift of the surface plasmon resonance peak was also reported towards a shorter wavelength in their copper-doped samples by increasing the ablation duration from 15 to 60 min at a fixed incident laser energy.[47] This shift was attributed to a reduction in the size of the formed nanoparticles as per transmission electron microscopy analyses. This observation supports the decrease in CuNPs size that was found in our study, as it significantly decreases with increasing irradiation dose (Table 3).

Studies on metal nanoparticles, such as Ag nanoclusters,[48] have shown that metallic particles formed under irradiation influence the local charge balance, promoting electron capture and hole recombination, according to the following reactions in the case of CuNPs:

$$\text{NBOHC} + e^- \rightarrow \text{NBO} \quad (15)$$

$$Cu^0 + \text{NBOHC} \rightarrow Cu^+ + \text{NBO} \quad (16)$$

These reactions suggest that NBOHCs act as charge donors, transferring electrons to CuNPs. This electron exchange reduces the number of optically active NBOHC sites, leading to a decrease in their optical absorbance as CuNPs grow.

However, in our present study, this expected suppression does not immediately occur. When irradiating from 1 to 100 kGy, both the NBOHC band and the CuNP surface plasmon resonance (SPR) band increase simultaneously. This suggests that at these doses, CuNPs and NBOHCs coexist and grow together, rather than CuNPs directly quenching the NBOHC signal. It is only when the dose reaches 1000 kGy that both bands begin to decrease, indicating that at this extreme dose, CuNPs finally begin to suppress the optical signals from NBOHCs likely due to a stronger charge transfer effect and the saturation of defect formation.

In this study, isochronous annealing of the gamma-irradiated sample at 100 kGy for 30 minutes at temperatures ranging from 60 °C to 500 °C revealed significant changes in optical absorption properties (Fig. 6). At lower annealing temperatures (60 °C), a significant reduction in optical absorption intensity of the HC_1, HC_2 and SPR bands was observed, indicating the initial relaxation of defects. As the temperature increased to 300 °C, the absorbance continued to decline, reflecting further defect stabilization within the glass matrix. Beyond 300 °C, the optical absorption plateaued, suggesting that the system reaches a thermally stable state, where further annealing does not significantly affect the optical properties. The CuNPs size exhibited a characteristic growth trend (Table 4), reaching a maximum of 7.96 nm at 350 °C. However, beyond this point, a slight decrease in size was observed (7.84 nm at 450 °C, 7.49 nm at 500 °C), suggesting a near-saturation in growth. Factors such as particle coalescence, sintering, and matrix stabilization likely contributed to this behaviour, preventing further substantial size increases.

Indeed, when annealing the ion-exchanged samples, the Cu^0 formed during the ion-exchange process itself and/or after irradiation tended to coalesce and aggregate, forming larger nanoparticles. This coalescence process consumed the initially available number of Cu^0, reducing the number of distinct nanoparticles while increasing their average size. This decrease in the total number of plasmonic oscillators leads to lower SPR intensity, as fewer particles contribute to plasmon resonance. Additionally, as particle size increases, the mean free path of conduction electrons becomes longer, causing broader and weaker SPR peaks, which dampens the overall plasmonic response. This phenomenon is consistent with previous studies on metallic nanoparticles embedded in glass, such as those by Manikandan *et al.*[13]

A similar trend has been observed in silver nanocomposites, where thermally-induced clustering reduces SPR intensity.[49] This reduction is closely linked to structural stabilization, as nanoparticles transition from a highly dispersed state to larger, more stable aggregates. Consequently, further nanoparticle growth is limited, and their optical properties shift, making CuNPs less responsive to plasmonic excitation at elevated temperatures.

Another contributing factor in the observed decrease in SPR intensity was the recombination of NBOHCs, a well-documented phenomenon in the literature at elevated temperatures, according to the dominance of the oxidation-driven reaction mentioned in eqn (10), which became dominant when further increasing the temperature:[50]

$$\text{NBOHC} + Cu^+ \rightarrow Cu^{2+} + \text{NBO}$$

EPR analysis (Fig. 8) confirmed this trend, showing an increasing Cu^{2+} signal alongside a decreasing NBOHC signal. This process consumes Cu^+ ions, reducing their availability for further Cu^0 formation and thereby slowing CuNP growth.

These findings indicate that the observed SPR intensity decrease is driven not only by particle coalescence and electron scattering effects but also by chemical interactions within the glass matrix that influence the availability of Cu species for plasmonic activity.

In our study, and in contrast to the usual correlation where a blue shift is linked to a decrease in particle size, we observed a blue shift despite an increase in NP size. This phenomenon can be attributed to the significant decrease in full width at half maximum (FWHM) values as the cluster size increases, as detailed in Table 4. The reduction in FWHM with larger clusters was well-documented in previous research[13] indicating a clear size dependency of the plasmon resonance width. This decrease in FWHM with increasing cluster size is primarily influenced by the mean free path effect, which becomes prominent for smaller clusters ($R \leq 10$ nm).

Building on the results from isochronous annealing, we further explored the effects of isothermal annealing on the gamma-irradiated samples (Fig. 8). By keeping the temperature constant at 600 °C, while varying the annealing durations (60–180 min), we investigated how the defects and nanoparticles evolve over time under stable thermal conditions. It was observed that this annealing approach progressively reduces the SPR peak intensity while enhancing the Cu_2O NP band at 490 nm, with prolonged heating (up to 180 minutes) leading to the complete disappearance of the SPR peak and stabilization of the Cu_2O absorbance. This indicates the full oxidation of CuNPs into Cu_2O NPs.

Notably, high-dose irradiation generates a substantial number of defects, such as oxygen vacancies and interstitials, within the glass matrix and Cu NPs. These defects enhance oxygen diffusion and Cu ion mobility, accelerating the oxidation of metallic Cu to Cu_2O. As Cu oxidizes, the metallic core, responsible for the collective oscillation of conduction electrons that produces the SPR band, is consumed. The resulting Cu_2O lacks the free electrons necessary to sustain plasmonic resonance, leading to the disappearance of the SPR band.

In contrast, non-irradiated samples oxidize more slowly through diffusion-driven mechanisms, allowing metallic Cu to remain and sustain the SPR band for longer durations, as observed in Fig. 3.

The saturation of the Cu_2O band at 440 nm in irradiated samples signifies the formation of a dense Cu_2O layer that limits further oxidation, aligning with the complete loss of the SPR band due to the absence of metallic Cu.[51]

Additionally, the irradiation-induced energy deposition also causes fragmentation and size reduction of the nanoparticles.[52] Smaller nanoparticles, with their higher surface area-to-volume ratio, oxidize more rapidly, further accelerating the transformation into Cu_2O. The interplay between oxidation, fragmentation, and diffusion processes ensures that the smaller Cu NPs are fully consumed, stabilizing Cu_2O as the dominant phase.

In a study from 2011, the synthesis of colloidal copper nanocrystals and their solvent-dependent oxidation to form Cu_2O nanoparticles were investigated, in which an almost similar behavior of disappearance of the surface plasmon resonance (SPR) peak and the dominance of Cu_2O optical features was observed.[53] A rapid oxidation leading to a reduction in the metal domain size (replaced by semiconducting copper oxide shells) just occurred upon removing the synthesized Cu nanocrystals from an oxygen-free mixture and diluting them in an oxygenated solvent. The plasmon intensity decreased during oxidation, disappearing when the metal nanocrystals shrank below a few nanometers (as such small particles do not exhibit plasmon responses). This effect was only observed at longer oxidation times; however, at the earlier stages of oxidation, an increase in both the SPR and Cu_2O bands was observed.

In our study, the annealing of an irradiated Cu-doped sample (1000 kGy) at 600 °C for an extended duration (180 min) results in the presence of only Cu_2O NPs, with a complete disappearance of CuNPs. To our knowledge, this finding has not been previously reported in the literature on copper-doped glass silicates. The transformation from CuNPs to Cu_2O alters the material's properties significantly, influencing its potential applications. The disappearance of surface plasmon resonance (SPR) eliminates plasmonic effects that enhance light absorption; however, the semiconducting nature of Cu_2O still facilitates efficient light capture. This aligns with the assumption that Cu_2O, as a p-type semiconductor with a band gap of ~2 eV and a high optical absorption coefficient, is well-suited for solar energy conversion applications.[54]

Compared to CuNPs, which are easily oxidized, Cu_2O nanoparticles exhibit superior stability, making them more environmentally friendly and chemically robust for long-term use. Additionally, their compatibility with polymers enables the fabrication of diverse composite materials.[55] Therefore, this transition from CuNPs to Cu_2O NPs presents both challenges and opportunities, particularly in fields such as optoelectronics, photovoltaics, and sensor technology.[56,57]

Conclusions

Copper doped glass was obtained by a Cu^+–Na^+ ion-exchange process. Glass samples were then subjected to gamma rays and/or to thermal annealing in air. It was found that a small fraction of the monovalent copper diffused ions were reduced to Cu^0 atoms during the ion exchange process, giving rise to the appearance of a surface plasmon resonance (SPR) peak. Increasing the post thermal annealing duration of the as-exchanged glass samples led to an increase in the volume fraction of the CuNPs in the glass matrix, as evidenced by the increased SPR intensity. Thermally treated Cu^+–Na^+ exchanged glass samples at 600 °C resulted in the formation of Cu_2O NPs, with significantly higher absorbance intensity observed in samples subjected to prolonged heat treatment (180 min). Irradiating the Cu exchanged glass samples at doses up to 100 kGy greatly enhanced the SPR peak intensity, suggesting increased formation and volume fraction of CuNPs. On the other hand, irradiation with higher doses (1000 kGy) led to a significant decrease in SPR intensity and

a blue shift of ~15 nm, indicating a reduction in nanoparticle size. Isothermal annealing of the already irradiated samples at 1000 kGy reduces the SPR peak intensity while enhancing the Cu_2O NP band, with prolonged heating (up to 180 minutes) leading to the complete disappearance of the SPR peak and stabilization of the Cu_2O absorbance. This indicates that the full oxidation of CuNPs into Cu_2O NPs occurs only if the samples were irradiated before undergoing thermal annealing. This study provides valuable insights into the slight differences that could be introduced in the optical and adsorption properties of Cu^+–Na^+ exchanged glass through controlled thermal annealing and irradiation. Particularly, understanding the relationship between treatment parameters such as annealing duration, temperature, and irradiation dose and their effect on nanoparticle formation and plasmonic behavior is critical for advancing applications in photonics, optoelectronics, and sensing technologies.

Data availability

The authors declare that all data are available upon request from the corresponding authors.

Author contributions

Conceptualization, S. T. and K. F.; methodology, S. T. and K. F.; software, S. T.; validation, K. F. and A. A.; formal analysis, K. F.; investigation, S. T. and K. F.; resources, K. F. and A. A.; data curation, S. T. and K. F.; writing – original, S. T. and A. A.; writing – review and editing, A. A.; visualization, A. A.; supervision, K. F. and A. A.; project administration, K. F.; funding acquisition, A. A. All authors have read and agreed to the published version of the manuscript.

Conflicts of interest

There are no conflicts to declare.

Acknowledgements

We would like to thank Centre National des Sciences et Technologies Nucléaires (CNSTN), Tunisia, for granting us access to the 60Co gamma irradiation facilities. A. A. acknowledges SYSTAM's group fund received from the Spanish Ministry of Science and Innovation (MCI-21-PID2020-113558RB-C41), and her individual scientific funds received from the Spanish Ministry of Science and Innovation, namely PTA2021-020817-I and RYC2022-038426-I.

References

1 A. L. Stepanov, Nonlinear optical properties of metal nanoparticles in silicate glass, *Glass Nanocomposites*, 2016, pp. 165–179.
2 Y. X. Zhang and Y. H. Wang, Nonlinear optical properties of metal nanoparticles: a review, *RSC Adv.*, 2017, **7**(71), 45129–45144.
3 N. Pellerin, J. P. Blondeau, S. Noui, M. Allix, S. Ory, O. Veron and D. Massiot, Control of selective silicate glass coloration by gold metallic nanoparticles: structural investigation, growth mechanisms, and plasmon resonance modelization, *Gold Bull.*, 2013, **46**(4), 243–255.
4 M. Alqathami, A. Blencowe, U. J. Yeo, S. J. Doran, G. Qiao and M. Geso, Novel multicompartment 3-dimensional radiochromic radiation dosimeters for nanoparticle-enhanced radiation therapy dosimetry, *Int. J. Radiat. Oncol., Biol., Phys.*, 2012, **84**(4), e549–e555.
5 P. Retif, S. Pinel, M. Toussaint, C. Frochot, R. Chouikrat, T. Bastogne and M. Barberi-Heyob, Nanoparticles for radiation therapy enhancement: the key parameters, *Theranostics*, 2015, **5**(9), 1030.
6 G. K. Inwati, Y. Rao and M. Singh, Situfreeradicalgrowthmechanism of platinum nanoparticles by microwave irradiation and electro-catalytic properties, *Nanoscale Res. Lett.*, 2016, **11**, 458.
7 D. A. Giljohann, D. S. Seferos, W. L. Daniel, M. D. Massich, P. C. Patel and C. A. Mirkin, Gold nanoparticles for biology and medicine, *Angew. Chem., Int. Ed.*, 2010, **49**, 3280–3294.
8 X. Liu, Colloidal plasmonic nanoparticles for ultrafast optical switching and laser pulse generation, *Front. Mater.*, 2018, **5**, 59.
9 O. Véron, J.-P. Blondeau, D. De Sousa Meneses and C. A. Vignolle, Characterization of silver or copper nanoparticles embedded in soda-lime glass after a staining process, *Surf. Coat. Technol.*, 2013, **227**, 48–57.
10 R. Magruder, L. Yang, R. F. Haglund Jr., C. W. White, L. Yang and R. Dorsinville, *et al.*, Optical properties of gold nanocluster com posites formed by deep ion implantation in silica, *Appl. Phys. Lett.*, 1993, **62**, 1730–1733.
11 H. Tsuji, S. Kido, Y. Gotoh and J. Ishikawa, Negative-ion implanter for powders andits application to nanometer-sized metal par ticle formation in the surface of glass beads, *Rev. Sci. Instrum.*, 2000, **71**, 804–806.
12 S. Karlsson, Modification of float glass surfaces by ion exchange, *Doctoral Dissertation*, School of School of Engineering of Linnaeus University, Sweden, 2012.
13 P. Manikandan, D. Manikandan, E. Manikandan and A. Christy Ferdinand, Structural, optical and micro-raman scatter ing studies of nanosized copper ion (Cu+) exchanged soda limeglasses, *Plasmonics*, 2014, **9**, 637–643.
14 I. G. Kumar, P. Kumar, W. D. Roos, H. C. Swart and M. Singh, UV irradiation effects on tuning LSPR of Cu/Ag nanoclusters in ion exchanged glass matrix and its thermodynamic behavior, *J. Alloys Compd.*, 2020, **823**, 153820.
15 J. Zhang, W. Dong, J. Sheng, J. Zheng, J. Li, L. Qiao and L. Jiang, Silver nanoclusters formation in ion-exchanged glasses by thermal annealing, UV-laser and X-ray irradiation, *J. Cryst. Growth*, 2008, **310**(1), 234–239.
16 K. Farah, F. Hosni, A. Mejri, B. Boizot, A. H. Hamzaoui and H. B. Ouada, Effect of gamma rays absorbed doses and heat treatment on the optical absorption spectra of silver ion-

exchanged silicate glass, *Nucl. Instrum. Methods Phys. Res., Sect. B*, 2014, **323**, 36–41.
17 S. Toumi, A. Adawy, A. Quaranta and K. Farah, Copper nanoparticle and point defect formation in Cu+–Na+ ion-exchanged glass using protons of 2 MeV energy, *Dalton Trans.*, 2024, **53**(22), 9578–9589.
18 S. Karlsson, Modification of float glass surfaces by ion exchange, *Doctoral Dissertation*, School of School of Engineering of Linnaeus University, Sweden, 2012.
19 K. Farah, T. Jerbi, F. Kuntz and A. Kovacs, Dose measurements for characterization of a semi-industrial cobalt-60 gamma-irradiation facility, *Radiat. Meas.*, 2006, **41**(2), 201–208.
20 S. Toumi, A. Adawy, A. Quaranta and K. Farah, Exploiting Cu^{+}–Na^{+} ion-exchanged and Ar/H_2 annealed glass matrix to synthesize copper nanoparticles, *J. Am. Ceram. Soc.*, 2024, **107**(11), e1–e18.
21 P. Kumar, M. C. Mathpal and H. C. Swart, Multifunctional properties of plasmonic Cu nanoparticles embedded in a glass matrix and their thermodynamic behavior, *J. Alloys Compd.*, 2018, **747**, 530–542.
22 J. Zhang and J. Sheng, Formation and optical properties of copper nanoclusters in a silicate glass, *Int. J. Hydrogen Energy*, 2009, **34**(8), 3531–3534.
23 S. Palomba, L. Novotny and R. E. Palmer, Blue-shifted plasmon resonance of individual size-selected gold nanoparticles, *Opt. Commun.*, 2008, **281**(3), 480–483.
24 O. A. Yeshchenko, I. M. Dmitruk, A. M. Dmytruk and A. A. Alexeenko, Influence of annealing conditions on size and optical properties of copper nanoparticles embedded in silica matrix, *Mater. Sci. Eng., B*, 2007, **137**(1–3), 247–254.
25 J. Sheng, K. Kadono, Y. Utagawa and T. Yazawa, X-ray irradiation on the soda-lime container glass, *Appl. Radiat. Isot.*, 2002, **56**(4), 621–626.
26 A. Bishay, *J. Non-Cryst. Solids*, 1970, **3**, 54–114.
27 E. J. Friebele, in *Radiation effects, Optical properties of glass*, ed. D. R. Uhlmann and N. J. Kreidl, Westerville, 1991, pp. 205–261.
28 C. D. Marshall, J. A. Speth and S. A. Payne, *J. Non-Cryst. Solids*, 1997, **212**, 59–73.
29 D. L. Griscom and M. Mizuguchi, *J. Non-Cryst. Solids*, 1998, **239**, 66–277.
30 Q. Wang, H. Geng, C. Sun, Z. Zhang and S. He, *Nucl. Instrum. Methods Phys. Res., Sect. B*, 2010, **268**, 1478–1481.
31 T. S. Buys and K. De Clerk, Bi-Gaussian fitting of skewed peaks, *Anal. Chem.*, 1972, **44**(7), 1273–1275.
32 S. I. Andronenko, R. R. Andronenko, A. V. Vasilev and O. A. Zagrebel'nyi, *Glass Phys. Chem.*, 2004, **30**, 230–235.
33 S. Toumi and K. Farah, Thermoluminescent response of gamma irradiated Na+–Cu+ ion-exchanged silicate glass in large dose range, *Nucl. Sci. Tech.*, 2023, **34**(5), 66.
34 B. Boizot, F. Y. Olivier, G. Petite and D. Ghaleb, Blocking of alkaline migration under ionizing irradiation in Cr-doped oxide glasses, *Nucl. Instrum. Methods Phys. Res., Sect. B*, 2008, **266**(12–13), 2966–2970.
35 P. D. Johnson and F. E. Williams, Specific magnetic susceptibilities and related properties of manganese activated zinc fluoride, *J. Chem. Phys.*, 1950, **18**, 322.
36 S. I. Andronenko, R. R. Andronenko and A. V. Vasilev, *et al.*, Local symmetry of Cu2+ ions in sodium silicate glasses from data of EPR spectroscopy, *Glass Phys. Chem.*, 2004, **30**, 230–235, DOI: **10.1023/B:GPAC.0000032224.23793.8c**.
37 J. M. Dance, J. P. Darnaudery and H. Baudry, *et al.*, Etude par RPE de verres appartenant au système Cao-B2O3-AL2O3 dopés a V4, Fe3+ et Cu2+, *Solid State Commun.*, 1981, **39**, l99–l120.
38 R. J. Araujo, S. Likitvanichkul, Y. Thibault and D. C. Allan, Ion exchange equilibria between glass and molten salts, *J. Non-Cryst. Solids*, 2003, **318**(3), 262–267.
39 F. Gonella, F. Caccavale, L. D. Bogomolova, F. d'Acapito and A. Quaranta, Experimental study of copper–alkali ion exchange in glass, *J. Appl. Phys.*, 1998, **83**(3), 1200–1206.
40 A. Quaranta, E. Cattaruzza and F. Gonella, Modelling the ion exchange process in glass: phenomenological approaches and perspectives, *Mater. Sci. Eng., B*, 2008, **149**(2), 133–139.
41 B. Messerschmidt, C. H. Hsieh, B. L. McIntyre and S. N. Houde-Walter, Ionic mobility in an ion exchanged silver—sodium boroaluminosilicate glass for micro-optics applications, *J. Non-Cryst. Solids*, 1997, **217**(2–3), 264–271.
42 D. Manikandan, S. Mohan, P. Magudapathy and K. G. Nair, Irradiation induced dissolution of Cu and growth of Ag nanoclusters in Cu/Ag ion-exchanged soda-lime glass, *Nucl. Instrum. Methods Phys. Res., Sect. B*, 2002, **198**(1–2), 73–76.
43 G. K. Inwati, Y. Rao and M. Singh, Thermodynamically induced in situ and tunable Cu plasmonic behaviour, *Sci. Rep.*, 2018, **8**(1), 3006.
44 P. Kumar, M. C. Mathpal, S. Ghosh, G. K. Inwati, J. R. Maze, M. M. Duvenhage, W. D. Roos and H. C. Swart, Plasmonic Au nanoparticles embedded in glass: Study of TOF-SIMS, XPS and its enhanced antimicrobial activities, *J. Alloys Compd.*, 2022, **909**, 164789.
45 J. X. Xu, F. Ren, D. J. Fu and C. Z. Jiang, Effect of thermal annealing on the optical properties of low-energy Cu-implanted silica glass, *Phys. B*, 2006, **373**(2), 341–345.
46 O. I. Sallam, A. Alhodaib, S. Abd El Aal and F. M. Ezz-Eldin, Influence of gamma ray on optical and structural properties of commercial glass enriched with copper oxide, *Inorg. Chem. Commun.*, 2021, **124**, 108388.
47 P. K. Baruah, A. K. Sharma and A. Khare, Effective control of particle size, surface plasmon resonance and stoichiometry of Cu@ CuxO nanoparticles synthesized by laser ablation of Cu in distilled water, *Opt. Laser Technol.*, 2018, **108**, 574–582.
48 R. Espiau de Lamaestre, H. Béa, H. Bernas, J. Belloni and J. L. Marignier, Irradiation-induced Ag nanocluster nucleation in silicate glasses: Analogy with photography, *Phys. Rev. B: Condens. Matter Mater. Phys.*, 2007, **76**(20), 205431.
49 A. K. Pal and D. B. Mohan, SERS enhancement, sensitivity and homogeneity studies on bi-metallic Ag-Cu films through tuning of broad band SPR towards red region, *J. Alloys Compd.*, 2017, **698**, 460–468.
50 S. Sakka, K. Kamiya and K. Kato, Incorporation of copper into glass by the Cu□Na ion exchange, *J. Non-Cryst. Solids*, 1982, **52**(1–3), 77–90.
51 C. Ocal, S. Ferrer and N. Garcia, Cabrera-Mott mechanism for oxidation of metals explains diffusion of metallic atoms

through thin defective oxide layers, *Surf. Sci.*, 1985, **163**(2–3), 335–356.

52 G. Bongiovanni, P. K. Olshin, C. Yan, J. M. Voss, M. Drabbels and U. J. Lorenz, The fragmentation mechanism of gold nanoparticles in water under femtosecond laser irradiation, *Nanoscale Adv.*, 2021, **3**(18), 5277–5283.

53 K. P. Rice, E. J. Walker Jr., M. P. Stoykovich and A. E. Saunders, Solvent-dependent surface plasmon response and oxidation of copper nanocrystals, *J. Phys. Chem. C*, 2011, **115**(5), 1793–1799.

54 S. Nandy, A. Banerjee, E. Fortunato and R. Martins, A review on Cu2O and CuI-based p-type semiconducting transparent oxide materials: promising candidates for new generation oxide-based electronics, *Rev. Adv. Sci. Eng.*, 2013, **2**(4), 273–304.

55 X. Ma, S. Zhou, X. Xu and Q. Du, Copper-containing nanoparticles: Mechanism of antimicrobial effect and application in dentistry-a narrative review, *Front. Surg.*, 2022, **9**, 905892.

56 K. Thanigai Arul, E. Manikandan, R. Ladchumananandasivam and M. Maaza, Novel polyvinyl alcohol polymer based nanostructure with ferrites co-doped with nickel and cobalt ions for magneto-sensor application, *Polym. Int.*, 2016, **65**(12), 1482–1485.

57 T. Siva, S. Muralidharan, S. Sathiyanarayanan, E. Manikandan and M. Jayachandran, Enhanced polymer induced precipitation of polymorphous in calcium carbonate: calcite aragonite vaterite phases, *J. Inorg. Organomet. Polym. Mater.*, 2017, **27**, 770–778.